Thin Pellets: Fast Electrochemical Preparation of Capacitor Tantalum Powders

Tian Wu,[†] Xianbo Jin,*[,†] Wei Xiao,[†] Xiaohong Hu,[†] Dihua Wang,[†] and George Z. Chen*[,†,‡]

College of Chemistry and Molecular Sciences, Wuhan University, Wuhan, 430072, P. R. China, and School of Chemical, Environmental and Mining Engineering, University of Nottingham, University Park, Nottingham NG7 2RD, UK

Received August 8, 2006. Revised Manuscript Received October 19, 2006

Electrochemical reduction of solid Ta_2O_5 to Ta metal in molten $CaCl_2$ at 1123 K has been studied by cyclic voltammetry and potentiostatic electrolysis, together with spectroscopic, electron microscopic, and elemental analyses. The initial step in the electro-reduction process is the electrochemically driven oxide−Ca^{2+} interaction, leading to the formation of two or more stable calcium-containing compounds which are likely $Ca_{0.5}Ta_2O_5$ and $CaTa_2O_5$. These compounds are then reduced to TaO and/or δ-TaO before full metallization. At potentials more negative than −0.9 V vs Ag/AgCl, fine tantalum powder (aggregates of nodular ∼200 nm particles) can be prepared by direct electrolysis of thin and porous pellets of the Ta_2O_5 powder (aggregates of nodular particles of ∼300 nm in size). The current efficiency and energy consumption are satisfactory, for example, achieving ∼78% and ∼2.4 kWh/kg-Ta at −1.0 V, respectively. The oxygen concentration in the produced Ta powder can be reduced to as low as 1200 ppm by electrolysis at a cell voltage of 3.1 V for 10 h. The specific capacitance of the electrolytic Ta powder reaches 40 kμFV/g.

Introduction

Personal electronic devices, most noticeably mobile phones, have significantly changed our life style. This is, to a significant degree, due to the use of tantalum (Ta) capacitors which account for over 60% of the world's annual consumption of this unique metal.[1,2] At present, the Ta metal, mostly in the form of a fine powder, is commercially produced via many complex procedures, including two very costly steps: (1) extraction of Ta as a pure fluoride compound, K_2TaF_7, from the mineral, e.g., $Fe(TaO_3)_2$ which often coexists with $Fe(NbO_3)_2$, involving the use of hydrofluoric acid (HF) and methyl isobutyl ketone; (2) sodiothermic reduction of K_2TaF_7 to Ta powder in a molten salt bath containing fluoride (e.g., KCl + NaCl + NaF at about 1073 K) according to reaction 1.[1,2]

$$K_2TaF_7 + 5\ Na \rightleftharpoons Ta + 2\ KF + 5\ NaF \qquad (1)$$

This fluoride-based process has been a current industrial preference for its capability of direct production of Ta powders at a reasonably large scale and an acceptable cost, considering the rarity of the Ta mineral resource. However, the use of fluorides does impose safety and environmental concerns.

In fact, other Ta compounds, such as Ta_2O_5 and $TaCl_5$, can also be produced effectively from the same or similar mineral sources,[1,3−5] and many attempts to reduce these nonfluoride compounds by a direct or indirect metallothermic reduction route were described in the literature.[3−10] Particularly, the metallothermic reduction of Ta_2O_5 involved the use of an alkali or alkaline earth metal reductant (L = Na, Mg, or Ca in most cases) as represented by reaction 2.[6−10]

$$Ta_2O_5 + 5x\ L \rightleftharpoons 2\ Ta + 5\ L_xO \qquad (x = 2 \text{ or } 1) \qquad (2)$$

Note that the Ta_2O_5 is usually in the solid state (e.g., pure powder) in reaction 2, while the K_2TaF_7 in reaction 1 is dissolved in the molten salt. These metallothermic processes are usually highly exothermic, making it difficult to control the reaction when the system temperature reaches as high as 2273 K.[6] Further, the process can also be kinetically retarded because the byproduct, L_xO, may cover up the unreacted Ta_2O_5.[6] Performing reaction 2 in a molten chloride salt (e.g., $CaCl_2$ or LiCl) that can dissolve L_xO has been more effective for producing fine Ta particles (<1 μm), but the powder usually contains 4000−37000 ppm oxygen,[7−10] apparently due to the effect of the L_xO-enriched molten salt.

* Corresponding authors. (G.Z.C.) Tel: +44-115-9514171. Fax: +44-115-9514115. E-mail: george.chen@nottingham.ac.uk. (X.B.J.) Tel: +86-27-68756319. Fax: +86-27-68756319. E-mail: xbjin@whu.edu.cn.

† Wuhan University.

‡ University of Nottingham.

(1) Miller, G. L. *Tantalum and Niobium*; Butterworths Scientific Publications: London, 1959.

(2) Okabe, T. H.; Sadoway, D. R. *J. Mater. Res.* **1998**, *13*, 3372−3377.

(3) Park, I.; Okabe, T. H.; Waseda, Y. *J. Alloys Compd.* **1998**, *280*, 265−272.

(4) Park, I.; Okabe, T. H.; Lee, O. Y.; Lee, C. R.; Waseda, Y. *Mater. Trans. JIM* **2002**, *43*, 2080−2086.

(5) Mineta, K.; Okabe, T. H. *J. Phys. Chem. Solid.* **2005**, *66*, 318−321.

(6) Nersisyan, H. H.; Lee, J. H.; Lee, S. I.; Won, C. W. *Combust. Flame* **2003**, *135*, 539−545.

(7) He, J. L.; Pan, L. T.; Zheng, A. G.; Li, H. J. *Min. Res. Dev.* **2003**, *S1*, 6−8 (in Chinese).

(8) Baba, M.; Ono, Y.; Suzuki, R. O. *J. Phys. Chem. Solids* **2005**, *66*, 466−470.

(9) Baba, M.; Suzuki, R. O. *J. Alloys Compd.* **2005**, *392*, 225−230.

(10) Suzuki, R. O.; Baba, M.; Ono, Y.; Yamamoto, K. *J. Alloy. Compd.* **2005**, *389*, 310−316.

10.1021/cm0618648 CCC: $37.00
Published on Web 12/14/2006

This problem may be solved by carrying out electrolysis of the molten salt so that the L metal is not added but produced *in situ* at the cathode while simultaneous removal of oxygen is achieved at the anode.[11−13] This electro-metallothermic reduction process can be further illustrated by reactions 3 and 4, including reaction 2 as the intermediate step.

$$2/m\ L^{m+} + 2\ e \rightleftharpoons 2/m\ L \qquad \text{(cathode, } m = 1 \text{ or } 2\text{)} \quad (3)$$

$$Ta_2O_5 + 5x\ L \rightleftharpoons 2\ Ta + 5\ L_xO \qquad (x = 2 \text{ or } 1;\ mx = 2) \quad (2)$$

$$C + y\ O^{2-}\ (\text{or } y\ L_xO) \rightleftharpoons CO_y + 2y\ e\ (+xy\ L^{x+}) \qquad \text{(carbon anode, } y = 1 \text{ or } 2\text{)} \quad (4)$$

According to thermodynamics, reactions 2 and 3 are equivalent to reaction 5 below:

$$Ta_2O_5 + 5x\ L^{m+} + 10\ e \rightleftharpoons 2\ Ta + 5\ L_xO\ \text{(cathode)} \quad (5)$$

This thermodynamic simplification is practically important because reaction 5 implies that reaction 3 could be unnecessary, and hence a lower energy input (less negative potential in terms of electrochemistry) may suffice for the reduction. Furthermore, if L_xO is completely dissociated into the L^{m+} and O^{2-} ions in the molten salt, reaction 5 can be further simplified to reaction 6.

$$Ta_2O_5 + 10\ e \rightleftharpoons 2\ Ta + 5\ O^{2-}\ \text{(cathode)} \quad (6)$$

Reactions 5 and 6 can be rewritten for other metal oxides and are known as "electro-deoxidation" or "electro-reduction" which has been applied to reduce a number of oxides, including those of Ti, Nb, Cr, Si, U, and Tb.[14−24]

Experimentally, in electro-reduction, the cathodic current collector is electrically attached to the oxide feed in the form of a porous preform such as pellets, but in electro-metallothermic reduction, electric contact is absent to the oxide feed for which a feed of powder is preferred. (If electric contact is present to the oxide feed, the latter becomes experimentally the same as the former.) In electro-metallothermic reduction, the presence of the metallic reductant means significant electronic conduction through the molten salt, leading to very low current efficiency. Use of an oxide-based diaphragm, e.g., MgO, can in principle reduce electronic conduction, although the reductant such as Ca or Li can threaten the stability of the oxide diaphragm.

On the other hand, it is acknowledged that the one-step transfer of more than two electrons to each metal atom in the oxide phase, as represented by reaction 5 or 6, is likely an electrochemical challenge. Particularly, previous work on the electro-reduction of solid TiO_2 in molten $CaCl_2$ has highlighted the existence of complex intermediate steps that lead to the formation of various perovskite phases ($Ca_\delta TiO_x$, $x/\delta \geq 2$), which affected significantly the speed and efficiency of the process.[15,16]

For making Ta powders by electro-reduction,[25−28] very little is known about the mechanism, and, more importantly, there has not been any report on the properties of the electrolytic Ta powders for capacitor applications. Particularly, it was thought that the process involved solid-state reactions and hence would be low in both speed and efficiency.[27] This thought seems to agree with a recent study in which the electrolysis of small pellets of mixed oxide powders, including Nb_2O_5, lasted for up to 88 h to reach a satisfactory low level of oxygen in the produced metals.[17,18]

It should be pointed out that in all past studies on electro-reduction involving porous pellets of oxide powders,[14−24] the pellet thickness and porosity were found to be important factors affecting the process speed, mainly due to the removed oxygen ions having to diffuse through the molten salt contained in the pores of the pellet.[18,24] In particular, by extrapolation of experimental data, we have anticipated that if the thickness of an oxide pellet with 45% porosity is reduced to 1.5 mm or thinner, the electro-reduction speed and efficiency can both be significantly improved.[24]

Herein, we present novel experimental findings on the electro-reduction of thin porous Ta_2O_5 pellets (1.3∼1.5 mm thick) in molten $CaCl_2$. The reduction of these thin Ta_2O_5 pellets took only a few hours to give rise to an ultrafine Ta powder (particle size: ∼200 nm) with very low oxygen contents (∼2000 ppm). In many previous studies, a constant cell voltage was applied for the electro-reduction process, which makes it difficult to clarify whether or not metallic calcium is formed on the cathode during electrolysis.[14−24] In this work, the cathode potential was controlled and selected according to cyclic voltammetry of Ta_2O_5, which can ensure the absence of the deposition of metallic calcium and help in deriving the reduction mechanism. This operation also led to high current efficiency and low-energy consumption, for example, achieving ∼78% and ∼2.4 kWh/kg-Ta at −1.0 V vs Ag/AgCl, respectively. In addition, unprecedented results are reported from our tests of the electrolytic Ta powders in capacitors, showing the electro-reduction method to be indeed promising for replacing the fluoride-based sodiothermic reduction method.

2. Experimental Section

Cyclic voltammograms (CVs) of solid Ta_2O_5 in molten $CaCl_2$ were recorded using a thin oxide layer-coated Ta wire (99.95%,

(11) Suzuki, R. O.; Teranuma, K.; Ono, K. *Metall. Mater. Trans. B* **2003**, *34*, 287−295.
(12) Suzuki, R. O. *J. Phys. Chem. Solids* **2005**, *66*, 461−465.
(13) Seo, C. S.; Jeong, S. M.; Park, S. B.; Jung, J. Y.; Park, S. W.; Kim, S. H. *J. Chem. Eng. Jpn.* **2006**, *39*, 77−82.
(14) Chen, G. Z.; Fray, D. J.; Farthing, T. W. *Nature* **2000**, *407*, 361−364.
(15) Schwandt, C.; Fray, D. J. *Electrochim. Acta* **2005**, *51*, 66−76.
(16) Jiang, K.; Hu, X. H.; Ma, M.; Wang, D. H.; Qiu, G. H.; Jin, X. B.; Chen, G. Z. *Angew. Chem., Int. Ed.* **2006**, *45*, 428−432.
(17) Yan, X. Y.; Fray, D. J. *Adv. Funct. Mater.* **2005**, *15*, 1757−1761.
(18) Yan, X. Y.; Fray, D. J. *J. Electrochem. Soc.* **2005**, *152*, D12−21.
(19) Chen, G. Z.; Gordo, E.; Fray, D. J. *Metall. Mater. Trans. B* **2004**, *35*, 223−233.
(20) Gordo, E.; Chen, G. Z.; Fray, D. J. *Electrochim. Acta* **2004**, *49*, 2195−2208.
(21) Jin, X. B.; Gao, P.; Wang, D. H.; Hu, X. H.; Chen, G. Z. *Angew. Chem., Int. Ed.* **2004**, *43*, 733−736.
(22) Yasuda, K.; Nohira, T.; Amezawa, K.; Ogata, Y. H.; Ito, Y. *J. Electrochem. Soc.* **2005**, *152*, D69−D74.
(23) Sakamura, Y.; Kurata, M.; Inoue, T. *J. Electrochem. Soc.* **2005**, *152*, D69−D74.
(24) Wang, D. H.; Qiu, G. H.; Jin, X. B.; Hu, X. H.; Chen, G. Z. *Angew. Chem., Int. Ed.* **2006**, *45*, 2384−2388.
(25) Fray, D. J.; Farthing, T. W.; Chen, Z. PCT Patent WO9964638, 1998.
(26) Krishnan, A.; Lu, X. G.; Pal, U. B. *Scand. J. Metall.* **2005**, *34*, 293−301.

0.5 mm in diameter, Western Metallic Material Co., Ltd., China) as the working electrode. This electrode was prepared by thermal oxidization in the air at 1133 K for about 5 or 10 s.

The Ta_2O_5 powder (99.99%, 300 nm in average particle size, Zhuzhou Cemented Carbide Works Imp. & Exp. Company) was pressed (10 MPa) into a cylindrical pellet (~2.0 cm in diameter, 1.3−1.5 mm in thickness, ~1.7 g in mass, ~45% in porosity). The pellet was sintered in air at 1173 K for about 2 h and sandwiched between two molybdenum wire meshes to form an assembled cathode for potentiostatic electrolysis. The electrolyzed pellet was washed in tap water, 0.1 M HCl and distilled water, and then dried in vacuum at 353 K before further analyses.

The as-received analytical grade anhydrous $CaCl_2$ (96%, Silian Reagent Plant, Shanghai, China) was used to prepare the electrolyte. A graphite crucible containing the $CaCl_2$ was settled in a stainless steel reactor and dried in air at about 573 K for about 3 days, followed by further drying under vacuum at 723 K for 2 h. The reactor was then flushed by a continuous flow of high purity argon (99.999%, Minghui Gas Technology Co., Ltd, China), and the temperature was raised to 1123 K. Preelectrolysis of the molten salt was carried out at 2.7 V between a graphite rod anode and a nickel sheet cathode for about 12 h. This procedure was commonly applied in previous work as a more convenient and safer laboratory practice (compared with using dry HCl gas) for the satisfactory removal of the moisture and some redox active impurities from molten $CaCl_2$.[14−21] The use of nickel as the cathode in the preelectrolysis was to alloy with and remove Mg which was present at a level of ~0.3 wt % in the as-received anhydrous $CaCl_2$.[29,30] While the nickel foil was indeed found to be enriched with Mg by XRD analysis after preelectrolysis,[30] it is acknowledged that, at 2.7 V, the cathodic removal of the Mg^{2+} impurity is likely incomplete. This is because the process must be accompanied by the anodic discharge of the O^{2-} ion whose concentration in the thermally prepared molten $CaCl_2$ is limited and strongly dependent on the heating history. Indeed, as is shown later, in the preelectrolyzed molten $CaCl_2$ used in this work, the presence of trace Mg^{2+} was still detected by cyclic voltammetry, suggesting that only partial removal of Mg^{2+} was achieved after preelectrolysis.

In voltammetric and potentiostatic experiments, a quartz sealed Ag/AgCl reference electrode[31] and a graphite counter electrode were used. CVs were recorded on a computer-controlled CHI660A Electrochemical System (Shanghai Chenhua, China), while the potentiostatic electrolysis was controlled by a multichannel four-electrode potentiostat (Neware, China). Some of the reactants and products were characterized by X-ray diffraction spectroscopy (XRD) (X-ray 6000 with Cu $K_{\alpha 1}$ radiation at $\lambda = 1.5405$ Å, Shimadzu, Japan), X-ray photoelectron spectroscopy (XPS) (Kratos XSAM800, Japan), transmission electron microscopy (TEM) (JEM-2010, Japan), and scanning electron microscopy (SEM, Sirion, Hillsboro, OR, USA), with energy-dispersive X-ray analysis (EDX) (GENESIS 7000, EDAX, Mahwah, NJ, USA). The impurities were examined by the Materials Test and Inspection Research Institute of Wuhan Iron and Steel (Group) Corp. (Wuhan, China) using inductively coupled plasma atomic absorption spectroscopy (ICP-AAS) (Agilent 7500a, Japan) and inert gas fusion oxygen analysis (RO-416DR, LECO, St. Joseph, MI, USA).

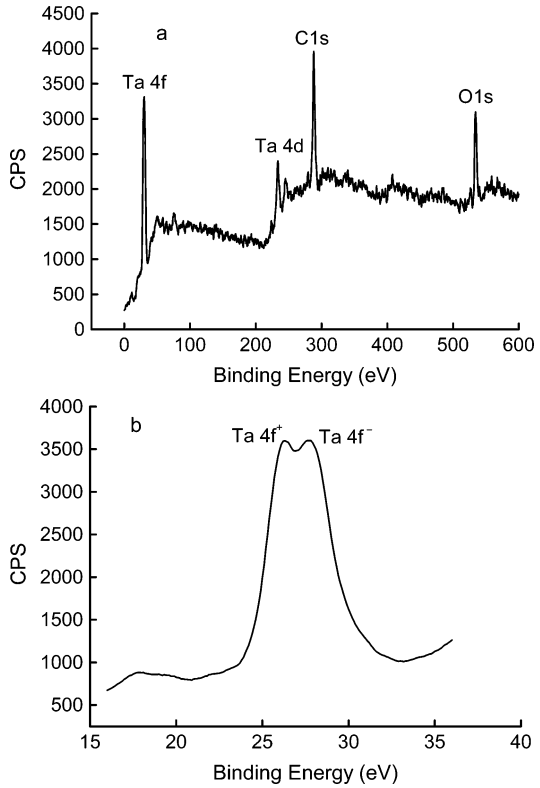

Figure 1. XPS spectra of the surface oxide layer on the tantalum wire formed at 1133 K for 10 s in air. (a) Wide scan. (b) High-resolution scan.

The obtained electrolytic Ta powder was made into the Ta capacitor anode (0.3−0.5 g per anode) via vacuum annealing at 1623 K and tested for capacitance according to a literature method.[32]

3. Results and Discussion

3.1. Cyclic Voltammograms of the Ta/Ta_2O_5 Electrodes. The wide scan XPS spectrum (Figure 1a) confirmed Ta and O to be the dominant elements in the thermally prepared oxide coating on the Ta wire, while the C peak was from the reference used. The high-resolution XPS spectrum recorded around the Ta peak at about 26 eV revealed two subpeaks (Figure 1b) as expected from the spin splitting of the 4f electrons of Ta.[33] The average binding energy of the two subpeaks is 26.9 eV which agrees well with that of Ta_2O_5 (26.7 eV). No other intermediate valences of Ta were found.

A typical cyclic voltammogram (CV) of the molten $CaCl_2$ used in this work is shown in Figure 2a (dashed line), recorded using a carefully cleaned molybdenum wire electrode at 1123 K. Between 0 and −1.0 V (vs Ag/AgCl) the CV shows small, slightly sloped, and paired parallel negative currents on the forward and backward potential scans. These currents were commonly observed in previous work in molten $CaCl_2$ and attributed to (1) charging/discharging of the electrode/electrolyte double-layer, and (2) electronic conduction through some redox active impurities (e.g., multivalent metal ions) in the molten salt.[14,29] The large reduction and reoxidation current peaks, labeled as D and

(27) Hu, X. F.; Xu, Q.; Wu, Y. *Mater. Rev.* **2005**, *19*, 97−99 (in Chinese).
(28) Hu, X. F.; Xu, Q. *Acta Metall. Sin.* **2006**, *42*, 285−289. (in Chinese)
(29) Qiu, G. H.; Ma, M.; Wang, D. H.; Jin, X. B.; Hu X. H.; Chen, G. Z. *J. Electrochem. Soc.* **2005**, *152*, E328−E336.
(30) Xiao, W.; Jin, X. B.; Deng, Y.; Wang, D. H.; Hu, X. H.; Chen, G. Z. *Chem. Phys. Chem.* **2006**, *7*, 1750−1758.
(31) Gao, P.; Jin, X. B.; Wang, D. H.; Hu, X. H.; Chen, G. Z. *J. Electroanal. Chem.* **2005**, *579*, 321−328.
(32) Li, C. G.; Gao, Y.; Dong, N. L. *J. Funct. Mater.* **2005**, *36*, 64−66. (in Chinese).
(33) Stickle, W. F.; Sobol, P. E.; Bomben, K. D. *Handbook of X-ray Photoelectron Spectroscopy (Kratos XSAM800)*; Perkin-Elmer Corporation Physical Electronics Division, 1992.

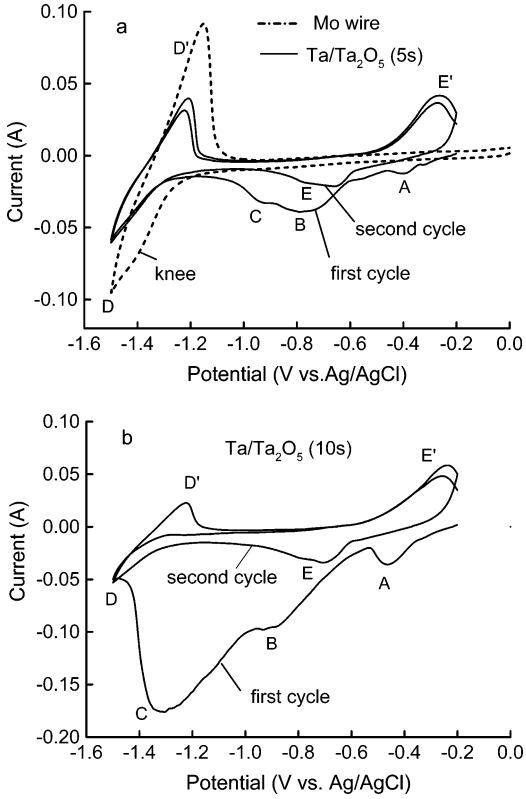

Figure 2. Cyclic voltammograms of thin Ta_2O_5 coatings on a Ta wire (diameter: 0.5 mm) prepared by thermal oxidation in air for (a) 5 s and (b) 10 s in molten $CaCl_2$ (1123 K). Potential scan rate: 100 mV/s.

D′ respectively, are indication of the reduction of the cations from the molten salt and the reoxidation (anodic dissolution) of the deposited metal.[14,21,29] As indicated in the Experimental Section, the molten $CaCl_2$ used in this work contained Mg^{2+} as impurity which could have only been partially removed by preelectrolysis with the nickel cathode. Therefore, the remaining Mg^{2+} ion could have been responsible for the knee seen on peak D at about −1.4 V, and the reduction current D might have contributions from not only the Ca^{2+} ion but also the impurity Mg^{2+} ion.[21,29] The product of peak D was thus likely an alloy of Ca and Mg whose anodic dissolution led to peak D′.

The CVs of the thermally formed Ta_2O_5 coating on the Ta wire in the same molten $CaCl_2$ are also presented in Figure 2a and 2b (solid line), showing reduction peaks A, B, C, D, E and reoxidation peaks D′ and E′. Apart from D and D′ whose origins have been discussed above, the appearance of multiple reduction peaks on the CVs of the Ta_2O_5 coating in a wide potential range (−0.2 V to −1.1 V) indicates the complexity of the electro-reduction of solid Ta_2O_5 in molten $CaCl_2$. On the Ta_2O_5 coating formed in 5 s oxidation in air at 1133 K, the CV of the first potential cycle shows at least three main reduction peaks (A, B, and C). However, only one reoxidation peak E′ was observed during the anodic potential scan, which was likely related to the anodic dissolution of Ta metal. The dissolved Ta species could be responsible for the only reduction peak E seen during the second potential cycle. When the oxidation time of the Ta wire increased to 10 s, peaks A, B, and C became more prominent (Figure 2b) with peak C showing the largest increase in current. While the current increase in all three

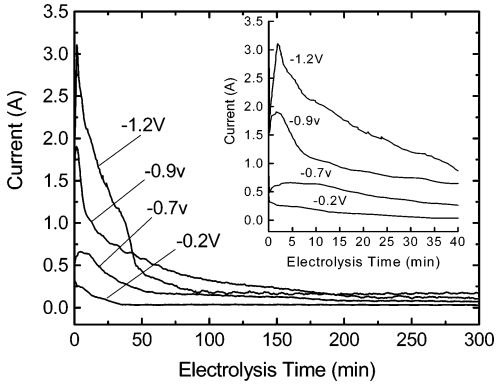

Figure 3. Typical current−time curves recorded during potentiostatic electrolysis of porous Ta_2O_5 pellets (∼1.66 g, 1.4 mm thick) at the indicated potentials (vs Ag/ AgCl) in molten $CaCl_2$ (1123 K). The insert shows the expanded portions in the first 40 min of electrolysis.

peaks reflects the increased amount (thickness) of the Ta_2O_5 coating, the significant negative shift of the peak potentials signifies a greater ohmic resistance in the thicker oxide coating. However, the similarities on the anodic branches and the second cycle CVs between Figure 2a and 2b are strong evidence that the Ta_2O_5 coatings were fully reduced after the first negative potential scan in both cases. In other words, the reduction of solid Ta_2O_5 is very fast even on the voltammetric time scale.

3.2. Potentiostatic Reduction of Thin Porous Ta_2O_5 Pellets. To understand the electro-reduction process represented by the afore-discussed CVs, a series of potentiostatic electrolysis of thin porous Ta_2O_5 pellets (1.3−1.5 mm thick) were carried out at different potentials in the range from −0.2 V to −1.3 V (cf. the potential range of CVs in Figure 2) at intervals of 0.1 V. All electrolysis experiments lasted for 5 h. Figure 3 shows typical current−time curves recorded during the electrolysis at some selected potentials.

It can be seen that negatively shifting the electrode potential led to larger reduction currents in the initial period (<40 min). At potentials between −0.2 V and −0.5 V where peak A appears on the CVs in both Figure 2a and 2b, the current−time curves had a similar shape to that of the −0.2 V curve in Figure 3. At more negative potentials, the electrolysis current went through three stages: a fast initial increase to a peak, a following slower decrease, and then a small but stable current, see in Figure 3. The initial current increase was commonly observed in previous work on electrolysis of porous pellets of oxides and can be accounted for by the charge (electrons + ions) transfer reactions occurring at the *metal* | *oxide* | *molten salt* three-phase lines (3PIs)[30,34] that expand from the initial *current collector* | *oxide* | *molten salt* three-phase contact points. When the surface of the oxide pellet was fully metallized, the reduction could only proceed into the interior of the pellet. Due to the increasing ohmic drop and concentration polarization with the 3PIs penetrating deeper into the pellet, the current decreased until the full reduction of the pellet.

In the whole period of electrolysis (5 h), the total charge passed increased with the potential becoming more negative

(34) Deng, Y.; Wang, D. H.; Xiao, W.; Jin, X. B.; Hu, X. H.; Chen, G. Z. *J. Phys. Chem. B* **2005**, *109*, 14043−14051.

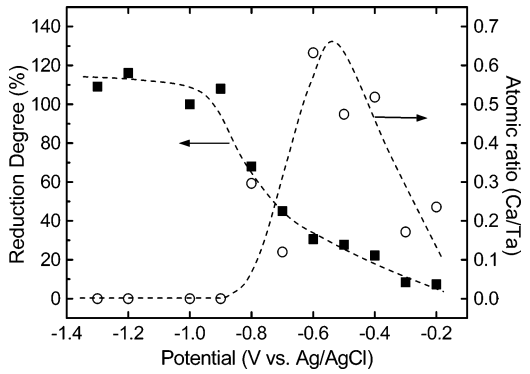

Figure 4. Reduction degree of the Ta_2O_5 estimated by coulometric analysis from Figure 3 (black squares) and the Ca/Ta atomic ratio calculated from the EDX measurement of the electrolysis products (open circles) in relation with the electro-reduction potential. The dashed lines are presented for viewing guidance only.

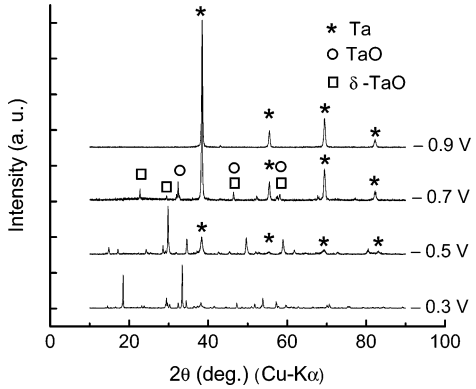

Figure 5. Typical XRD spectra of the electrolytic products from potentiostatic electrolysis of thin porous Ta_2O_5 pellets at the indicated potentials in molten $CaCl_2$ (5 h, 1123 K).

until −0.9 V. Afterward, the total charge passed remained approximately the same at different potentials. This behavior is understandable because the amount of Ta_2O_5 in each electrode was the same, and the total amount of charge needed to reduce the Ta_2O_5 should not be different. Note that, according to Figure 2a, −0.9 V falls in the potential range of peak C, suggesting this peak to be likely due to the formation of Ta metal.

The stable small currents at later electrolysis times were the same as or very similar to the residual current measured on the two bare molybdenum meshes. Excluding this stable (constant) residual current, the net reduction charge, Q_{net}, can be obtained by integrating the current−time curve for each applied potential. The mass of the pellet, m (=1.663 g), can also be converted to the reduction charge, Q_{mass}, according to the formula mass, M, of Ta_2O_5: $Q_{mass} = 10 \times 96500 \times m/M = 3631$ C for each pellet. The "reduction degree" is defined as $(Q_{net}/Q_{mass}) \times 100\%$, and is plotted in Figure 4 for each potential, showing clearly that the Ta_2O_5 pellet can be completely reduced to Ta metal within 5 h at potentials more negative than −0.9 V.

The products from electro-reduction of Ta_2O_5 at different potentials were first analyzed by SEM, EDX, and XRD. It should be mentioned that the samples were washed with water. Consequently, the products after washing would not contain substances that are soluble in or reactive with water. This is a concern particularly for Ca metal which is likely to form in electrolysis under constant cell voltage. However, because of the application of potentials much more positive than that for Ca deposition, the absence of Ca metal was ensured in the potentiostatically prepared samples in this work.

At potentials more negative than −0.9 V, only Ta was detected in the sample by EDX, indicating the complete reduction of the Ta_2O_5 pellets. From −0.2 V to −0.8 V, the respective EDX spectra showed clearly the presence of O, Ca, and Ta, indicating partial reduction. The morphologies of these partially reduced samples were complex, but it was noticed that these intermediate phases were electronically conducting because the SEM inspections revealed no charging effect on the bare samples. Conducting phases containing Ca and O or the perovskite phases, $Ca_\delta TiO_x$ ($x/\delta \geq 2$), were also observed in the products from partial reduction of TiO_2.[14,15] While EDX analysis of oxygen is limited in accuracy, it does confirm the presence of oxygen and hence indicates the detected Ca to be more likely in the cationic state. Interestingly, the more reliably detected amount of Ca reached a peak at about −0.6 V as shown in Figure 4 which plots the atomic ratio of Ca/Ta measured by EDX against the applied potential. No Ca was observed at potentials more negative than −0.9 V. (The oxygen level was also found to be lower than the detection limit of EDX, i.e., < 1%.) These observations suggest that the electro-reduction of solid Ta_2O_5 in molten $CaCl_2$ goes through an initial stage of electrochemically driven interaction between the solid oxide and calcium (Ca^{2+}), rather than solely oxygen removal. The oxide−Ca^{2+} interaction could be either Ca^{2+} insertion (with little structure change) or inclusion (with structural rearrangement) in the solid oxide phase, which is similar to what was found in the electro-reduction of TiO_2 in either molten $CaCl_2$[16] or molten LiCl.[35]

Figure 5 shows four typical XRD patterns of products from potentiostatic electrolysis at −0.3 V, −0.5 V, −0.7 V, and −0.9 V, respectively. In fact, these XRD patterns are representatives of the XRD patterns recorded in four different potential ranges, namely (1) −0.2 V ∼ −0.4 V, (2) −0.5 V ∼ −0.6 V, (3) −0.7 V ∼ −0.8 V, and (4) - 0.9 V ∼ −1.3 V. Efforts were made to identify each of these products, but only the XRD patterns at the two more negative potential ranges, i.e., 3 and 4, could be properly recognized. Particularly, the TaO and δ-TaO phases were seen at −0.7 V as intermediate products. Figure 5 shows clearly that Ta_2O_5 was completely reduced to Ta metal at −0.9 V, although a small amount of the metal could also form as early as −0.5 V. More discussion will be given later about this phenomenon, considering both kinetic and thermodynamic effects.

The unknown phases represented by the −0.3 V and −0.5 V XRD patterns may be derived from Figures 4 and 5. From the EDX results, the Ca/Ta atomic ratio was 0.18−0.25 at −0.2 V to −0.4 V and increased to 0.48−0.63 at −0.5 V to −0.6 V. The corresponding reduction degrees were 7−9% and 20−30%, respectively. The XRD patterns at these potentials suggested two stable phases which thus may be

(35) Jiang, K.; Hu, X. H.; Sun, H. J.; Wang, D. H.; Jin, X. B.; Ren, Y. Y.; Chen, G. Z. *Chem. Mater.* **2004**, *16*, 4324−4329.

assumed as $Ca_{0.5}Ta_2O_5$ (Figure 5, −0.3 V) and $CaTa_2O_5$ (Figure 5, −0.5 V) in which the atomic Ca/Ta ratios are 0.25 and 0.5 with the reduction degrees being 10% and 20%, respectively.

Based on these findings, the electro-reduction mechanism may be speculated as following in accordance with the above-discussed product phases identified by XRD and EDX analyses.

$$Ta_2O_5 + 0.5\,Ca^{2+} + e \rightleftharpoons Ca_{0.5}Ta_2O_5 \quad (7)$$

$$Ca_{0.5}Ta_2O_5 + 0.5\,Ca^{2+} + e \rightleftharpoons CaTa_2O_5 \quad (8)$$

$$CaTa_2O_5 + 4\,e \rightleftharpoons 2\,TaO + Ca^{2+} + 3\,O^{2-} \quad (9)$$

$$TaO + 2\,e \rightleftharpoons Ta + O^{2-} \quad (10)$$

It should be mentioned that, in agreement with reactions 7 and 8, mass increase was recorded in pellets electrolyzed at potentials between −0.2 V and −0.5 V. In addition, the calcium-containing phases may not always have well-defined stoichiometries as specified above, but a more general formula of $Ca_\delta TaO_{2.5-\gamma}$ ($0 \le \delta \le 2/3$, $0 \le \gamma \le 1.5$, as derived from the EDX results given in Figure 4), is not unreasonable. These $Ca_\delta TaO_{2.5-\gamma}$ phases could also be directly electro-reduced to the Ta metal in a manner similar to the following example.

$$CaTa_2O_5 + 8\,e \rightleftharpoons 2\,Ta + Ca^{2+} + 5\,O^{2-} \quad (11)$$

Thus, the reduction peaks on the CVs in Figure 2 can be assigned as reaction 7 to peak A, reaction 8 to peak B, reactions 9 and 10 or 11 to peak C, respectively. Although pure Ta was only obtained in the electrolysis products at potentials more negative than −0.9 V, a small amount of the Ta phase is shown on the −0.5 V XRD pattern in Figure 5. This observation is in fact thermodynamically possible, considering the following reaction 12,

$$Ta_2O_5 \rightleftharpoons 2\,Ta + 2.5\,O_2\,(g) \qquad (\Delta G^o = 1582\ \text{kJ at } 1123\ \text{K}) \quad (12)$$

which shows that Ta_2O_5 can be electro-decomposed at a voltage of 1.619 V at 1123 K as calculated from the Gibbs free energy change.[36] Under the same conditions, the decomposition voltage of CaO is 2.685 V. Therefore, against the same reference redox couple, for example, O_2/O^{2-}, the Ta metal could form at a much more positive potential than that for the electro-deposition of Ca.

However, this reduction mechanism, i.e., Ta_2O_5 directly to Ta without intermediate steps, seems to have contributed only slightly to the electro-reduction process performed in this work. It is likely that, at relatively less negative potentials, e.g., −0.5 V, reaction 12 could only occur at the pellet's surface where the O^{2-} ion can readily enter the bulk electrolyte. However, when the reduction proceeds to the interior of the pellet, the polarization on O^{2-} ion concentration will increase, and hence slows reaction 12. On the other hand, both reactions 7 and 8 can compete with reaction 12 to form the calcium-enriched solid phases, which are more stable than Ta_2O_5. Therefore, it is challenging to completely metallize the Ta_2O_5 pellet at relatively less negative potentials through reaction 12.

Figures 6a and 6b compare the SEM images of the as-received Ta_2O_5 powder and the electrolytic Ta powder. Both images reveal uniform particle sizes and similar nodular shapes, but the Ta particles are slightly smaller (300 nm-Ta_2O_5 vs 200 nm-Ta). This phenomenon differs from those observed in the electro-reduction of TiO_2, Nb_2O_5, and other oxides, in which the produced metal particles were a few or a few tens of micrometers in size, although the oxide feeds were also sub-micrometer particles. Ta has a melting point of 3253 K which is much higher than those of, for example, Ti (1943 K) and Nb (2741 K).[37] Therefore, the Ta particles were smaller than the Ta_2O_5 particles due to oxygen removal by electro-reduction, but the former could not grow very much because of the low electrolysis temperature. This fact suggests that even finer Ta particles may be achievable by either using smaller oxide particles and/or lowering the electrolysis temperature.

It is interesting to note that, similar to the interconnected nodular Ta_2O_5 particles in Figure 6a, the smaller nodular Ta particles in Figure 6b and 6c are also interconnected into larger aggregates (2−5 μm). Such structures are bifunctional: higher surface area and greater electronic conductivity for enhanced capacitance and reduced equivalent series resistance, respectively. From high-resolution TEM images, thin coatings (2−5 nm) could be recognized on the surface of the Ta particles (Figure 4d). These coatings should be Ta_2O_5 which might have formed during the postelectrolysis processing procedures, e.g., washing in water and drying in air, but also prevented the underneath Ta metal from further oxidation. Similar coatings were also observed on Ta particles produced by the sodiothermic reduction of K_2TaF_7.[38] The total oxygen contained in this thin coating was estimated, and the results suggested that the majority of oxygen measured from the powder was originated from the surface oxide layer, which in turn indicates that the as-electrolyzed Ta powder contained a very low level of oxygen.

The oxygen concentration in the electrolytic Ta powders was investigated against the electro-reduction time at −1.3 V (Figure 7). For the electrolysis of a ∼1.7 g Ta_2O_5 pellet, 99% Ta metal could be achieved in about 1 h and the oxygen concentration reduced to ∼2000 ppm in 5 h. This reduction speed is far greater than what was reported for the electro-reduction of Nb_2O_5 to Nb, where the oxygen concentration in the obtained Nb metal was as high as 7000 ppm even after electrolysis for 24 h under conditions very similar to those of this work.[18] This difference may be due to two important factors: first, thin oxide pellets were used in this work and the produced fine Ta particles did not grow very much in size. Both ensured high reduction speed by fast removal of the dissolved oxygen in the Ta particles and of

(36) Liang, Y. J.; Che, Y. C.; Liu, X. X.; Li, N. J. *Thermochemical Properties of Inorganic Substance*; Northeastern University Press: Shenyang, 1993 (in Chinese).

(37) Weast, R. C. *CRC Handbook of Chemistry and Physics*, 70th ed.; CRC Press: Inc.: Boca Raton, 1989−1990.

(38) He, J. L.; Pan, L. T.; Lu, Z. D.; Shi, W. F.; Shu, Y. C.; Zeng, F. P. *Ningxia Eng. Technol.* **2002**, *1*, 23−28 (in Chinese).

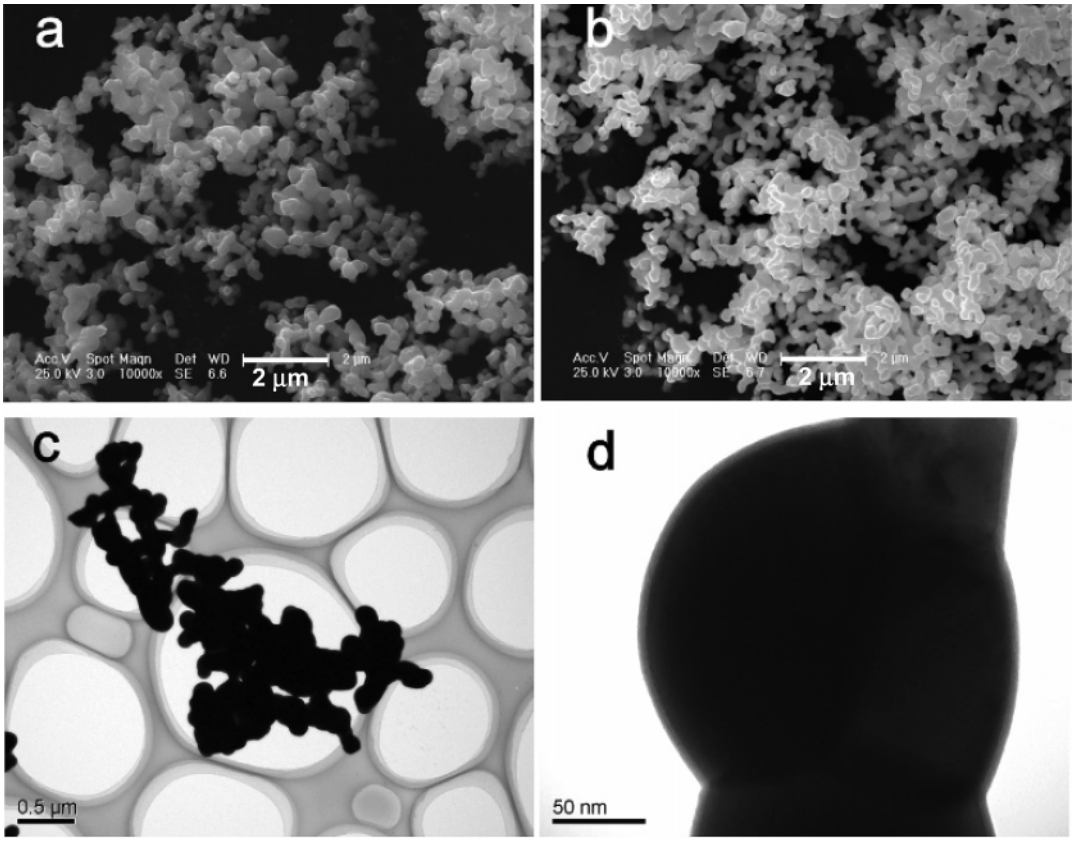

Figure 6. SEM images of (a) the as-received Ta_2O_5 powder, and (b) the electrolytic Ta powder whose details are shown by the TEM images in parts c and d.

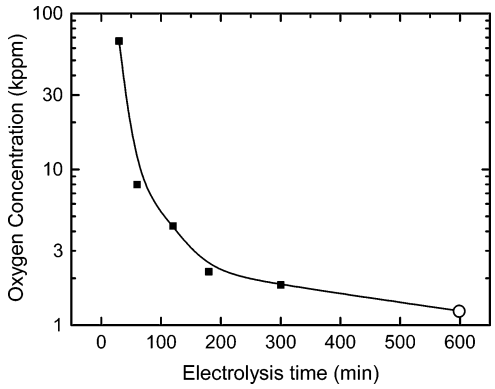

Figure 7. Oxygen concentrations in electrolytic Ta powders in relation to times for electrolysis of thin (~1.4 mm) porous Ta_2O_5 pellets in molten $CaCl_2$ (1123 K). Black squares: potentiostatic electrolysis at −1.3 V vs Ag/AgCl. Open circles: constant cell voltage electrolysis at 3.1V for 10 h.

the O^{2-} ions from the pellets during electrolysis. Second, the use of sub-micrometer Ta_2O_5 particles in this work (vs the 2−5 micrometer Nb_2O_5 particles used in the literature work[18]) could have also played a minor role. As shown in Figure 7, an oxygen concentration less than 1200 ppm was achieved after electrolysis at 3.1 V (constant cell voltage) for 10 h. This oxygen level is much lower than that in the products from calciothermic reduction in molten $CaCl_2$ (~5000 ppm)[7−10] or sodiothermic reduction in molten NaCl + KCl + KF (~4000 ppm)[39] using K_2TaF_7 as the feed.

Table 1. Specifications and Results of Capacitor Tests of the Electrolytic Ta Powder[a]

	anode number			
	1	2	3	4
mass of Ta power (mg)	478	475	302	298
anode diameter (mm)	5.4	5.4	5.4	5.4
anode length (mm)	3..5	3.4	2.1	2.1
anode density (g/cm^3)	5.9	5.9	6.2	6.2
capacitance (kμFV/g)	39.5	39.7	39.6	39.0
leakage current (μA)	200	250	300	250

[a] Electrolysis conditions: 3.1V in cell voltage, 10 h, 1123 K.

3.3. Capacitor Tests. According to the primary particle size (~200 nm), the produced Ta powder as described above should have a capacitance of 30 kμFV/g to 70 kμFV/g,[40] depending on the manufacturing procedure of the capacitor. In this work, ~30 g of electrolytic Ta powder were prepared from the thin Ta_2O_5 pellets by constant cell voltage electrolysis (3.1 V, 10 h, 1123 K), of which four Ta anodes were fabricated via vacuum annealing at 1350 °C and tested for capacitance according to the literature method.[32] Specifications of each electrode are listed in Table 1, and the average specific capacitance approaches 40 kμFV/g. This value is in line with the requirement of capacitor Ta powders.[9] Considering that the as-prepared electrolytic powder was used directly in the capacitor tests, the obtained capacitance values are highly satisfactory.

However, the results in Table 1 also show relatively large leakage currents. The cause was thought to be likely linked

(39) Liu, H. D.; Pan, L. T.; Cheng, Y. W.; Lu, Z. D.; Zheng, A. G.; Ma, Y. Z.; Wang, C. X.; Li, H. *Chin. J. Rare Met.* **2003**, *27*, 35−38. (in Chinese)

(40) Wang, D. X.; Wang, X. Z.; Zhong, J. M. *Ningxia Eng. Technol.* **2005**, *4*, 57−59 (in Chinese)

Table 2. Concentrations of Main Impurities in the Electrolytic Ta Powder[a]

O (ppm)	Mg (ppm)	Fe (ppm)	Ni (ppm)	C (ppm)
~1200	<10	80−130	30−40	620−1100

[a] Electrolysis conditions: 3.1 V in cell voltage, 10 h, 1123 K.

to the impurities in the powder. Therefore, elemental analysis of the Ta powder was performed by ICP-AAS, and the results are listed in Table 2. Sufficiently low levels of Mg, Fe, and Ni were detected, but the content of C much exceeded the specification (a few tens of ppm) for capacitor applications, which could have been responsible for the measured large leakage currents.

The source of carbon contamination can be tracked to the graphite anode. During electrolysis, the CO_2 generated on the anode can transport to the cathode through either the gas phase or the molten salt in which dissolution of CO_2 can occur readily via, for example, reaction with CaO to form the CO_3^{2-} species. The discharge of CO_2 or CO_3^{2-} at the cathode can lead to the formation of carbon which then contaminates the Ta metal. There may be several methods to reduce the carbon contamination, such as simply replacing the graphite anode with one made from inert materials. It is also possible to combine the electro-reduction process with the SOM process[17,26,41] in which a solid oxygen ion conducting membrane is used as the separator between the cathode and the anode. The anode is usually a noble metal and directly incorporated on the dry side (not in contact with the molten salt) of the membrane. The O^{2-} ions enter the membrane from the molten salt side and exit at the dry side where, in the absence of the molten salt, the O^{2-} ion is directly oxidized to the oxygen gas at the noble metal anode.

(41) Martin, A.; Lambertin, D.; Poignet, J.-C.; Allibert, M.; Bourges, G.; Pescayre, L.; Fouletier, J. *JOM* **2003**, *55*, 52−54.

4. Summary

Thin and porous Ta_2O_5 pellets can be facilely electro-reduced to fine Ta powders in molten $CaCl_2$ at a mild temperature (1123 K) and a cathodic potential (≤ -0.9 V vs Ag/AgCl) far more positive than that for calcium deposition (≤ -1.2 V vs Ag/AgCl). Studies by cyclic voltammetry and potentiostatic electrolysis show that before complete metallization of the oxide pellet, several calcium-enriched solid oxide phases with a likely general formula of $Ca_\delta TaO_{2.5-\gamma}$ ($0 \leq \delta \leq 2/3$, $0 \leq \gamma \leq 1.5$) were formed through an electrochemically driven oxide−Ca^{2+} interaction (either insertion or inclusion of the Ca^{2+} ion in the solid phase). The next intermediate product is TaO whose reduction leads to the Ta powder. The electrolytic Ta powders consist of sub-micrometer nodular particles (~200 nm) that are interconnected to larger aggregates (2−5 μm), and the oxygen concentration can be easily reduced to about 1200 ppm. This kind of Ta powders exhibits a specific capacitance close to 40 kμFV/g. The carbon content in the product from this work is still too high, but appropriate measures can be implemented. From the results and analyses presented here, it is anticipated that electrolytic Ta powders with higher capacitance can be achievable by using finer Ta_2O_5 powder as the feed material. A completely new, fast, and fluoride-free molten salt electrolytic process is foreseeable for commercial production of high quality Ta powders.

Acknowledgment. The authors are grateful to the Natural Science Foundation of China for financial support (Grant Nos: 20403012 and 20125308). X.B.J. and G.Z.C. thank the Royal Society for the 2005-06 China Fellowship.

CM0618648